Bioorganic & Medicinal Chemistry 18 (2010) 5995–6005

Contents lists available at ScienceDirect

Bioorganic & Medicinal Chemistry

journal homepage: www.elsevier.com/locate/bmc

Synthesis of aryl-heteroaryl ureas (AHUs) based on 4-aminoquinoline and their evaluation against the insulin-like growth factor receptor (IGF-1R)

William Engen [a], Terrence E. O'Brien [a], Brendan Kelly [a], Jacinda Do [a], Liezel Rillera [a], Lance K. Stapleton [b], Jack F. Youngren [b,*], Marc O. Anderson [a,*]

[a] Department of Chemistry & Biochemistry, San Francisco State University, 1600 Holloway Ave., San Francisco, CA 94132, USA
[b] Diabetes and Endocrine Research, University of California, San Francisco/Mt. Zion Medical Center, Box 1616, San Francisco, CA 94143-1616, USA

ARTICLE INFO

Article history:
Received 17 April 2010
Revised 18 June 2010
Accepted 21 June 2010
Available online 25 June 2010

Keywords:
Quinoline
Naphthyridine
2-Chloroquinoline
2-Quinolone
IGF-1R
Diaryl urea
Aryl heteroaryl urea
Insulin like growth factor receptor
Kinase inhibition
Pharmacophore based virtual screening

ABSTRACT

The insulin-like growth factor receptor (IGF-1R) is a receptor tyrosine kinase (RTK) involved in all stages of the development and propagation of breast and other cancers. The inhibition of IGF-1R by small molecules remains a promising strategy to treat cancer. Herein, we explore SAR around previously characterized lead compound (**1**), which is an aryl-heteroaryl urea (AHU) consisting of 4-aminoquinaldine and a substituted aromatic ring system. A library of novel AHU compounds was prepared based on derivatives of the 4-aminoquinoline heterocycle (including various 2-substituted derivatives, and naphthyridines). The compounds were screened for in vitro inhibitory activity against IGF-1R, and several compounds with improved activity (3–5 μM) were identified. Furthermore, a computational docking study was performed, which identifies a fairly consistent lowest energy mode of binding for the more-active set of inhibitors in this series, while the less-active inhibitors do not adopt a consistent mode of binding.

1. Introduction

The insulin-like growth factor (IGF) system is an attractive target for the development of new anti-cancer drugs.[1–4] The IGF system is composed of two ligands IGF-1 and IGF-2, as well as two IGF receptor systems (IGF-1R and IGF-2R), which, along with the homologous insulin receptor (IR), are members of the superfamily of transmembrane receptor tyrosine kinases (RTKs). The receptor IGF-1R is important in the normal growth and development processes.[5,6] Interestingly, the IGF system also plays a critical role in the development of breast and other cancers (particularly prostate), including malignant transformation, mitogenic growth, and anti-apoptotic activity.[7–11] IGF-1R is often over-expressed in a number of human tumors, including colon, pancreas, prostate, bladder, and kidney,[7,1] although the significance of IGF-1R expression levels on prognosis is still uncertain.[7] Several methods have been studied to inhibit the IGF system, including monoclonal antibodies targeting the receptor[12], an approach currently being evaluated in clinical trials.[13,14] Further approaches are the suppression of the IGF-1 ligands and binding proteins,[15–17] and also the development of small-molecule inhibitors of the IGF-1R kinase.[18,19,4,3,20] The development of clinically useful inhibitors of IGF-1R kinase is complicated by the high homology (84%) with IR kinase.[21] The inability of small molecule ATP-competitive inhibitors to differentiate between IR and IGF-1R was a strong initial concern due to potential hyperglycemic side-effects caused by inhibition of IR.[22,23] However, in vivo studies of dual IGF-1R/IR inhibitors have routinely shown minimal effects on blood glucose levels, despite some evidence of systemic insulin resistance.[24,25] In fact, the growing evidence that IR is involved in carcinogenesis itself[26,27], in particular due to the upregulation of its fetal isoform (IR-A), that is activated by IGF-II, indicates that dual IGF-1R/IR inhibition is ideal in order to fully block IGF signaling in cancer.[22,23]

Our overall goal is to explore the aryl-heteroaryl urea (AHU) scaffold in order to identify structurally simple small-molecule inhibitors of IGF-1R. Previously we characterized a specific AHU compound (**1**) as an in vitro and in vivo inhibitor of IGF-1R.[28] Subsequently we described a parallel synthetic approach to generate libraries of AHUs, along with preliminary results attempting to optimize AHU compounds for inhibitory activity against IGF-1R.[29] In our previous work, lead compound **1** was the starting point for optimization against a cell-based receptor tyrosine autophosphorylation assay (Fig. 1). This paper found that AHU compounds with a

* Corresponding authors. Tel.: +1 415 338 6494; fax: +1 415 405 0377 (M.O.A.).
E-mail address: marc@sfsu.edu (M.O. Anderson).

0968-0896/$ - see front matter © 2010 Elsevier Ltd. All rights reserved.
doi:10.1016/j.bmc.2010.06.071

diverse selection of aromatic and heteroaromatic ring systems (napthalenes, alternatively connected quinolines, benzimidazole, pyridines, and thioimidazole), produced compounds with little or no activity against IGF-1R, albeit in a cell based autophorphorylation assay (Eq. 1). Among the structurally diverse heterocycles incorporated into AHU compounds, the only one that maintained noticeable activity was 4-aminoquinaldine. Subsequently, we constructed a library of AHUs based on 4-aminoquinaldine,[29] that incorporated 37 different substituted aromatic rings (Eq. 2). A small collection of compounds were identified with noticeable activity below 30 μM, and four inhibitors were found to be similarly potent as lead compound **1**. While this study did not produce a significantly optimized inhibitor, it did help us establish a tentative pharmacophore model for aryl-heteroaryl ureas, notably the requirement of the 4-aminoquinoline ring system. Interestingly, 4-aminopyridine was not found to be a satisfactory replacement for 4-aminoquinoline.[29] Herein, we examine inhibitors containing a collection of heterocycles more closely related to 4-aminoquinoline, notably compounds with alternative substitution at the 2 position, and analogous heterocycles with additional nitrogen atoms in the quinoline ring system (e.g., 3-aminonaphthyridines).

Since our initial work on AHU compounds as inhibitors of IGF-1R, several useful inhibitor-bound X-ray co-crystal structures IGF-1R have been published, facilitating structure-based optimization of new inhibitors,[30,31] including a recent report of a inhibitor BMS-754807 which has entered clinical development.[32] Particularly useful in our project was the structure of a potent benzimidazole scaffold bound to the unactivated IGF-1R kinase.[33] As described herein, we have found that the more active inhibitors in our library possess a consistent mode of binding when docked into the unactivated kinase structure, while the less potent inhibitors dock in multiple, somewhat arbitrary, binding modes.

2. Results and discussion

Based on our previous work identifying the need of the 4-aminoquinoline structural framework in this class of inhibitors[29], we chose to investigate new classes of inhibitors that incorporate analogs of this heterocyclic system (Fig. 2). In contrast to the commercially available heteroaromatic ring systems explored in our previous work,[29] the new classes of ring systems were either highly expensive or not available. The heteroaryl ring systems **3**{a} depicted in Figure 2 were chosen due to the presence of the general 4-aminoquinoline framework with additional structural features which may act to enhance binding with the postulated ATP binding site of the kinase, particularly nearby polar amino acid residues. Some of the features that were explored were electronically variable substituents at the 2 position, in **3**{2–4}, and additional heteroaryl nitrogen atoms in the napthyridine **3**{5 and 7} and tetrahydronapthyridine **3**{6} ring systems. The set of substituted aromatic ring systems **4**{b} evaluated in this series was designed based on our previous work targeting IGF-1R,[29] and we also added three heterocycle-linked aromatic systems, that is, the aryl-linked pyrimidine **4**{8–9} and 6-methylpyrazine **4**{10} frameworks, due to their presence in commercially-available isocyanates. We hypothesized that these latter three classes of substituted aromatic ring systems may enhance aqueous solubility of the final inhibitor structures due to their additional hydrogen-bond accepting atoms.

The synthesis of aryl-heteroaryl ureas **2**{a,b} is accomplished by the reaction of an amino heterocycle **3**{a} with substituted aryl isocyanate **4**{b} (Fig. 3). The formation of an undesired symmetrical urea byproduct **5**{b} has been a consistent problem, most likely due to the transient hydrolysis of aryl isocyanates (and decarboxylation) followed by coupling with another molecule of isocyanate. This competitive side-reaction seems to be especially problematic due to the poor nucleophilicity and slower reactivity of the intended heteroaromatic amine nucleophiles. The addition of strong base to enhance the nucleophilicity of heteroaromatic amines has been helpful in certain cases, but symmetrical urea formation still remains a problem. An added complication is the difficulty in purifying desired ureas from symmetrical ureas. Silica-gel chromatography is often difficult, even for products well separated by TLC, due to the tendency of symmetrical ureas to precipitate on silica columns, causing the impurity to 'bleed through' and contaminate the desired product. Nevertheless, we have found that crystallization and preparative RP-HPLC seem to consistently remove most symmetrical urea contamination from inhibitor samples, generating compounds of sufficient purity for screening. Yields from the urea coupling reaction were highly variable, ranging from 5% to 80%. The lower yields were generally accounted for by non-optimized precipitation procedures, designed to recover enough product simply for in vitro screening. Purification of the desired product from undesired symmetrical urea also accounts for lower isolated yield of compounds.

The synthesis of a series of 4-amino-2-trifluoromethylquinoline aryl-heteroaryl ureas is illustrated in Scheme 1. 4-Chloro-2-trifluoromethylquinoline (**6**) was treated with sodium azide to generate 4-azidoquinoline **7**, which was reduced by catalytic hydrogenolysis to generate aminoquinoline **3**{2}, and which was then coupled with a selection of substituted aromatic isocyanates to generate a library of aryl-heteroaryl ureas **2**{2,b} (see Table 1). In this case,

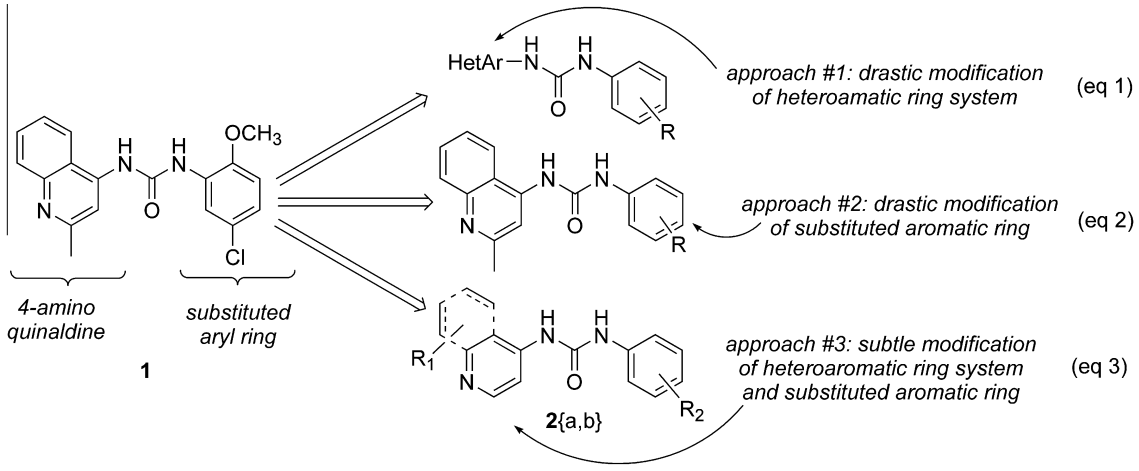

Figure 1. Design of novel aryl-heteroaryl ureas (AHUs) based on lead scaffold **1**. This publication focuses on the approach outlined in Eq. 3.

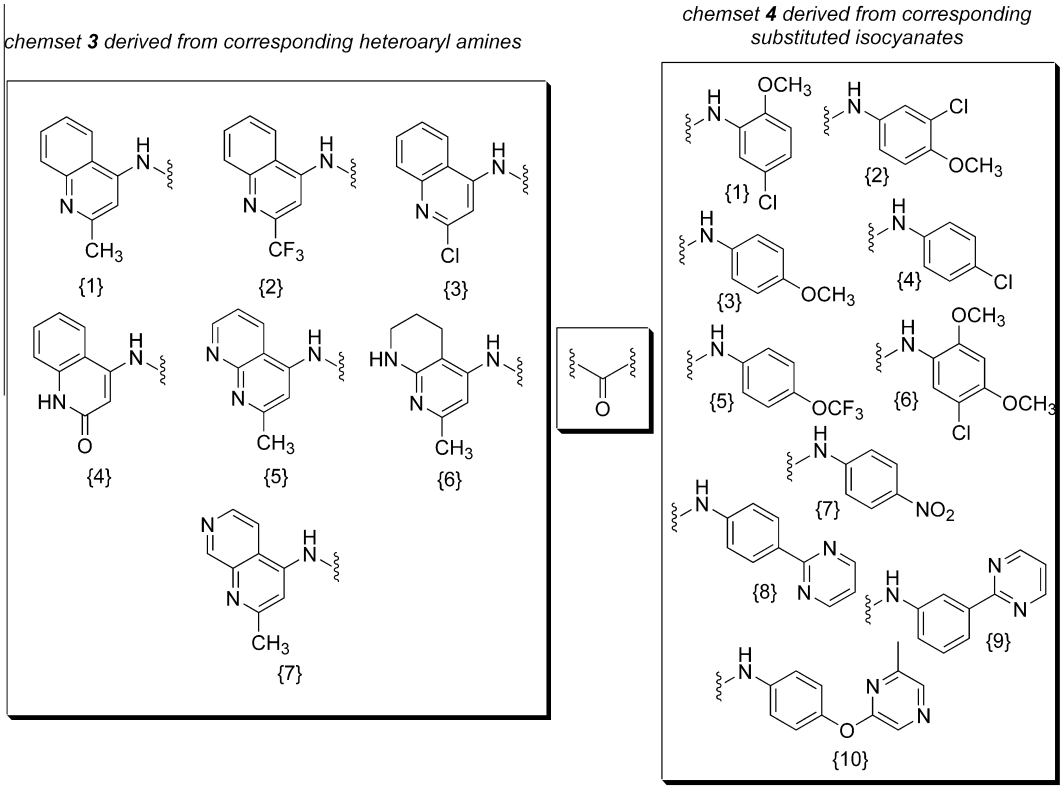

Figure 2. Overview of aryl-heteroaryl urea library derived from heteroaryl amine chemset **3** and substituted aryl chemset **4**. The composition of the library is outlined in Table 1.

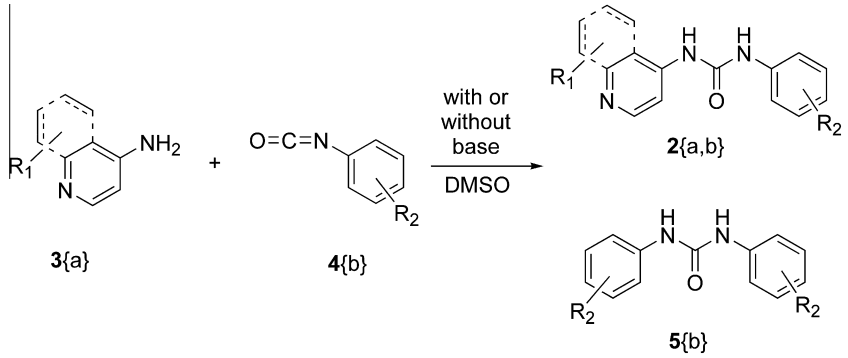

Figure 3. Synthesis of aryl-heteroaryl ureas **2**{a,b} and undesired formation of symmetrical ureas **5**{b}.

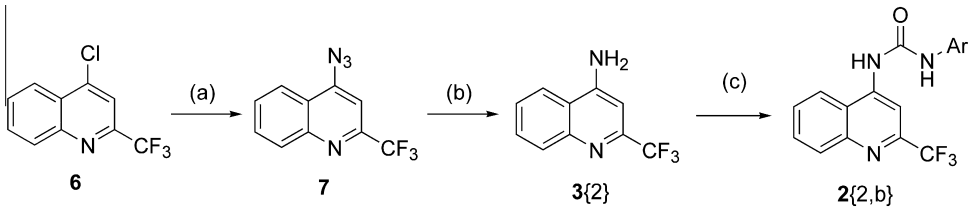

Scheme 1. Synthesis of aryl-heteroaryl ureas derived from 4-amino-2-trifluoromethylquinoline. Reagents and conditions: (a) NaN_3, 15-crown-5, 1-butanol; (b) H_2, Pd/C, CH_3OH; (c) Ar-NCO, NaO*t*Bu, DMSO.

the **3**{2} was poorly nucleophilic, and we found that the coupling was more effective in the presence of 2 equiv of sodium *tert*-butoxide.

The synthesis of AHUs derived from 4-amino-2-methyl-1,8-napthyridine and 4-amino-2-methyl-1,8-tetrahydronaphthyridine is shown in Scheme 2. Our first attempt, based on the classical Knorr and Conrad–Limpach reactions was unsuccessful. Hence, 2-aminopyridine (**8**) was transformed to imine **9**, while subsequent cyclization to **10** and then to **11** was unsuccessful. Instead, an alternative product (**12**) was found, as described previously.[34] An

Table 1
In vitro kinase inhibition screening results

Entry	Heterocyclic amine	Aryl isocyanate	Product	IGF-1R in vitro kinase inhibition (IC_{50} μM) (error)	*c* Log *P* determined in MarvinView (ChemAxon)
1	**3**{1}	**4**{1}	**2**{1,1}	18.7 (3.0)	3.85
2	**3**{1}	**4**{2}	**2**{1,2}	>30	3.85
3	**3**{1}	**4**{3}	**2**{1,3}	13.9 (4.5)	3.25
4	**3**{1}	**4**{4}	**2**{1,4}	>30	4.01
5	**3**{1}	**4**{5}	**2**{1,5}	>30	4.84
6	**3**{1}	**4**{8}	**2**{1,8}	>30	4.09
7	**3**{1}	**4**{9}	**2**{1,9}	>30	4.09
8	**3**{1}	**4**{10}	**2**{1,10}	5.6 (1.64)	3.20
9	**3**{2}	**4**{1}	**2**{2,1}	3.5 (0.72)	4.99
10	**3**{2}	**4**{2}	**2**{2,2}	8.8 (1.5)	4.99
11	**3**{2}	**4**{3}	**2**{2,3}	>30	4.38
12	**3**{2}	**4**{4}	**2**{2,4}	28.1 (5.0)	5.14
13	**3**{2}	**4**{5}	**2**{2,5}	6.7 (1.1)	5.97
14	**3**{2}	**4**{6}	**2**{2,6}	15.4 (4.1)	4.83
15	**3**{2}	**4**{7}	**2**{2,7}	27.1 (4.2)	4.48
16	**3**{2}	**4**{8}	**2**{2,8}	19.3 (5.2)	5.16
17	**3**{2}	**4**{9}	**2**{2,9}	>30	5.16
18	**3**{2}	**4**{10}	**2**{2,10}	5.2 (2.3)	4.33
19	**3**{3}	**4**{1}	**2**{3,1}	14.9 (5.3)	4.55
20	**3**{3}	**4**{2}	**2**{3,2}	>30	4.55
21	**3**{3}	**4**{3}	**2**{3,3}	>30	3.94
22	**3**{3}	**4**{4}	**2**{3,4}	21.1 (7.0)	4.70
23	**3**{3}	**4**{5}	**2**{3,5}	21.4 (11.9)	5.53
24	**3**{3}	**4**{8}	**2**{3,8}	>30	4.75
25	**3**{3}	**4**{9}	**2**{3,9}	>30	4.75
26	**3**{3}	**4**{10}	**2**{3,10}	>30	3.89
27	**3**{4}	**4**{1}	**2**{4,1}	6.5 (0.8)	2.38
28	**3**{5}	**4**{1}	**2**{5,1}	24.7 (7.6)	2.96
29	**3**{5}	**4**{10}	**2**{5,10}	12.5 (3.3)	2.31
30	**3**{6}	**4**{1}	**2**{6,1}	20.5 (7.1)	2.38
31	**3**{7}	**4**{1}	**2**{7,1}	>30	2.64
32	**3**{7}	**4**{6}	**2**{7,6}	>30	2.48

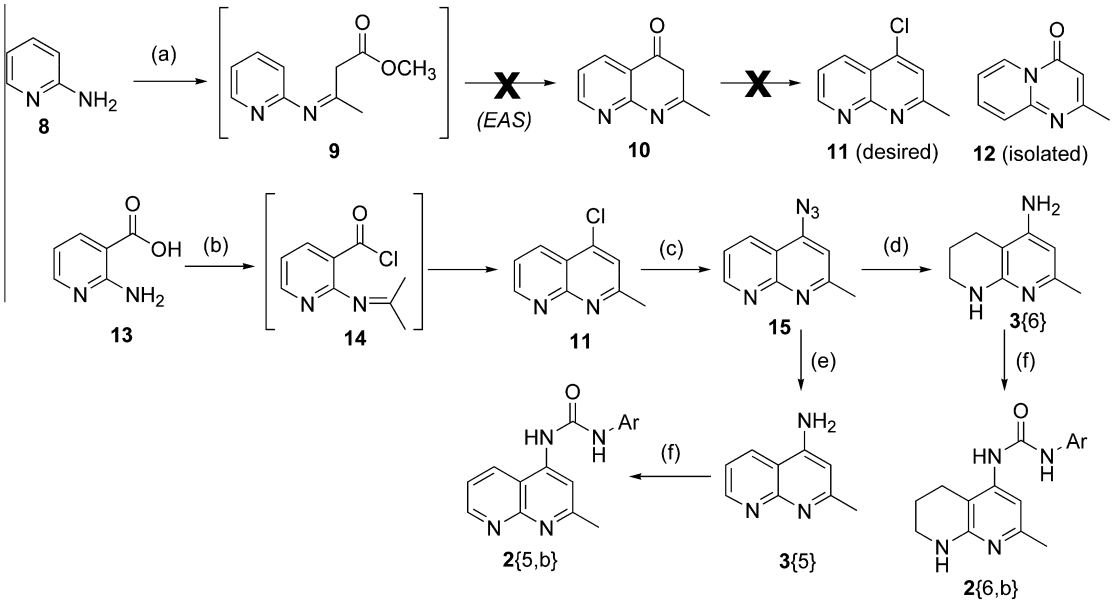

Scheme 2. Synthesis of aryl-heteroaryl ureas derived from 4-amino-1,8-napthyridine and 4-amino-1,8-tetrahydronapthyridine. Reagents and conditions: (a) methyl acetoacetate, $POCl_3$; (b) acetone, $POCl_3$; (c) NaN_3, 15-crown-5, CH_3OH; (d) H_2, cat. PtO_2 or Pd/C; (e) $NaBH_4$, CH_3OH; (f) Ar-NCO, DMSO.

alternative approach to 4-amino-1,8-naphthyridines begins with 2-aminonicotinic acid (**13**), which upon treatment with $POCl_3$ forms intermediate **14**, which then cyclizes to generate the desired heterocycle **11**. Conversion to the azide (**15**) was carried out smoothly. Attempted reduction of the azide through catalytic hydrogenolysis generated over-reduced tetrahydro-1,8-naphthyridine **3**{6} instead. Screening of alternative conditions to perform this reduction showed that sodium borohydride could carry out the desired azide reduction selectively to provide the desired 4-amino-1,8-naphthyridine ring system **3**{5}. Coupling of **3**{5} and

3{6} to aromatic isocyanates was done smoothly to generate AHUs **2**{5,b} and **2**{6,b}. The isocyanate coupling of these amines was affected efficiently without the addition of base.

After preparing 4-amino-2-methyl-1,8-naphthyridine **3**{5}, we attempted to explore the generality of this method to prepare other 4-aminonapththyridine-derived AHUs (Scheme 3). Thus we found that 3-aminoisonicotinic acid (**16**) could be cleanly converted to 4-chloro-2-methyl-1,7-naphthyridine (**17**) by treatment with acetone and $POCl_3$. The 4-chloronaphthyridine was then easily transformed to azide **18**, which was then selectively reduced to 4-amino-2-methyl-1,7-naphthyridine **3**{7}, and subsequently coupled to generate AHU compounds **2**{7,b}. Extension of this methodology to generate 4-chloro-2-methyl-1,6-naphthyridine (**20**) from 4-aminoisonicotinic acid (**19**) or from 4-aminopyridine (**21**) (Conrad–Limpach method) was unsuccessful.

In Scheme 4, the synthesis of two final scaffolds related to 4-aminoquinoline are presented. 2,4-dihydroxyquinoline (**22**) was readily converted to 2,4-dichloroquinoline (**23**). This molecule could be selectively hydrolyzed to the quinolin-2-one species (**24**) by treatment with aqueous acid, which was then transformed to azide **25**. The azide could then either be chlorinated again followed by azide reduction to generate 4-amino-2-chloroquinoline **3**{3} or directly reduced to generate 4-amino-quinolin-2-one **3**{4}. These two species were subsequently coupled to form respective AHU compounds **2**{3,b} or **2**{4,b}. In the case of **2**{4,b}, separation of the AHU product from symmetrical urea **5**{b} was rather difficult, and only one library member in this class could successfully be produced in high purity: **2**{4,1}.

Once the library of new AHU compounds was constructed, each compound was screened to determine in vitro inhibitory potency against the substrate tyrosine phosphorylation activity of purified IGF-1R kinase domain proteins. IC_{50} values were calculated from ELISA assays that measured tyrosine phosphorylation of immunocaptured substrates following incubation with purified IGF-1R and a range of AHU concentrations (Table 1). Additionally *c* Log *P* values were determined for each library member. Entries 2–8 are based on the lead inhibitor **2**{1,1} (entry 1), containing heteroaryl scaffold 4-aminoquinaldine **3**{1}. Entry 8 showed modest improvement in inhibitory potency, compared to the lead structure (entry 1). Entry 8 contains the 6-methylpiperazine heterocycle, which was incorporated to potentially improve aqueous solubility of the inhibitor (reflected by a lower *c* Log *P* value than other members in the series).

The first new class of AHU compounds described in this study were the 2-trifluoromethylquinolines **2**{2,b} (entries 9–18). Comparing entry 9 with the lead structure (entry 1), which are identical other than the 2-substituent on the quinoline, shows that entry 9 has obtained a fivefold improvement of inhibitory potency. Another entry with a modest improvement in potency compared to the lead structure was 4-trifluoromethoxyphenyl derivative (entry 13), which is greatly improved over the analogous 4-aminoquinaldine-derived inhibitor which was inactive (entry 5). Entry 18, containing the 6-methylpyrazine system **4**{10} was noticeably more potent than the lead structure (entry 1), and similar in potency to the 4-aminoquinaldine-derived analog (entry 8). As before, the hydrogen bond accepting 6-methylpiperazine heterocycle in Entry 18 most likely contributed to a decreased *c* Log *P* value compared to other compounds in this series.

The next class of AHU compounds to be examined were the 2-chloroquinoline AHU inhibitors **2**{3,b} (entries 19–26). In general, this class of inhibitors did not possess notable inhibitory activity against IGF-1R. Entry 19 was the most potent in the 2-chloroquinoline series, which had slightly improved potency when compared to the lead structure (entry 1), which also contains the 2-methoxy-5-chlorophenyl ring system.

A single inhibitor containing the 2-quinolone scaffold **3**{4} (entry 27) did display modestly improved activity in comparison with the lead structure (entry 1). Unfortunately, elaboration of a larger library of compounds in this series was complicated by poor nucleophilicity of the heterocycle with isocyanates, combined with exceptional difficulty in purifying products from symmetrical urea byproducts **5**{b}, by standard methods. The relatively low *c* Log *P* value could indicate improved aqueous solubility for this inhibitor, relative to the other inhibitors.

The remaining inhibitor scaffolds, based on 1,8-naphthyridine **2**{5,b} (entries 28–29), 1,8-tetrahydronaphthyridine **2**{6,b} (entry 30), and 1,7-naphthyridine **2**{7,b} (entries 31–32), possessed fairly low inhibitory potency compared to the lead structure (entry 1), and were not pursued further in this study. Entry 29, based on the aryl-linked 6-methylpyrazine ring system **4**{10} did possess slightly improved potency when compared to the lead structure (entry 1).

Overall, the 2-trifluoromethylquinoline scaffold **2**{2,b} could possibly represent more promising quinoline framework for AHU inhibitors of IGF-1R, given the enhanced potency of this series compared to 4-aminoquinaldine scaffold **2**{1,b}. Interestingly, the aryl-linked 2-methylpyrazine ring system **4**{10} seems to be present in a few of the more potent inhibitors (entries 8, 18, 29), and which is characterized by a relatively low *c* Log *P* value. However, an inhibitor containing a combination of 2-trifluoromethylquinoline and the 2-methylpyrazine systems (entry 18) did not achieve enhanced potency compared to the simpler 5-chloro-2-methoxy system (entry 9), suggesting these two features are not synergistic.

Given this new library of compounds with varying degrees of inhibitory activity against IGF-1R, we decided to establish a tentative binding model employing computational docking. We chose to dock AHU inhibitors into the ATP-binding site of IGF-1R kinase, the likely site of binding, with the OpenEyes ligand docking utility

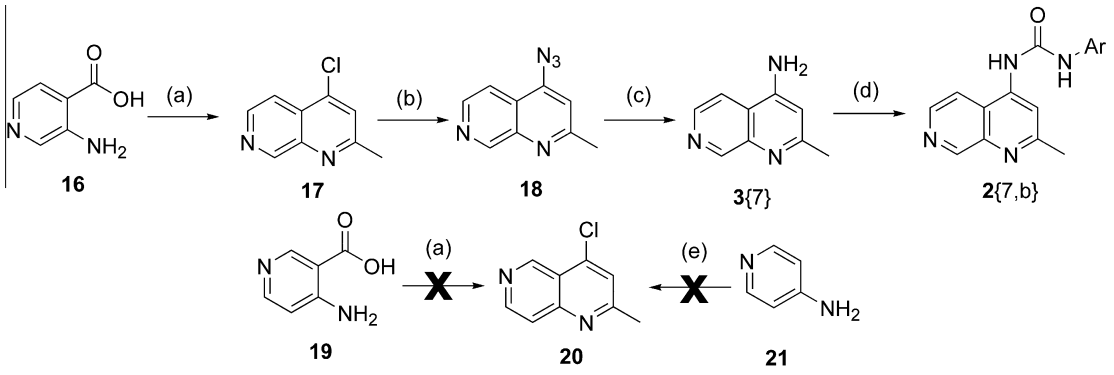

Scheme 3. Synthesis of aryl-heteroaryl ureas derived from 4-amino-1,7-napthyridine. Reagents and conditions: (a) acetone, $POCl_3$; (b) NaN_3, 15-crown-5, CH_3OH; (c) H_2, cat. PtO_2; (d) aryl isocyanate, DMSO; (e) ethyl acetoacetate, $POCl_3$.

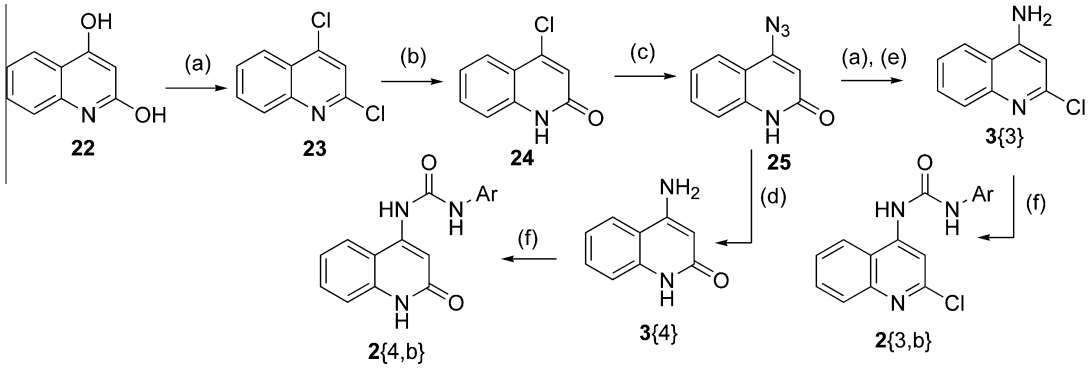

Scheme 4. Synthesis of aryl-heteroaryl ureas derived from 4-amino-2-chloroquinoline and 4-amino-2-oxoquinoline. Reagents and conditions: (a) $POCl_3$; (b) aq HCl, 1,4-dioxane; (c) NaN_3, 15-crown-5, CH_3OH; (d) H_2, Pd/C, CH_3OH; (e) $NaBH_4$, CH_3OH; (f) Ar-NCO, DMSO.

FRED. Our initial docking studies were carried out with a structure of the activated IGF-1R kinase, co-crystallized with a substrate peptide and ATP-mimic (PDB = 1K3A).[35] Unfortunately, using this structure there was little consistency with the mode of docking and potency of the inhibitors. We then obtained more satisfactory docking results using the co-crystal structure of a 3-(1*H*-benzo[*d*]imidazol-2-yl)pyridin-2(1*H*)-one lead compound with unactivated IGF-1R kinase (PDB = 2OJ9).[33]

Using the unactivated IGF-1R kinase structure, a number of our relatively potent AHU compounds produced relatively consistent poses where the quinoline heteroaryl nitrogen atom is poised to interact with Lys^{1003}. An example of this binding mode is illustrated in the lowest-energy pose of the most potent compound in this series, **2**{2,1}, shown in Figure 4 ('Binding Mode A'). In this model the quinoline carbocycle fits into a pocket surrounded by non-polar residues Val^{1023} and Val^{983}. A key set of interactions that may explain the enhanced potency of the **2**{2,b} series of inhibitors, are potential electrostatic contacts between the 2-trifluoromethyl group and Ser^{979} (backbone NH) and Thr^{1127} (sidechain OH). These interactions could explain the improved activity of **2**{2,1} versus the closely related lead structure **2**{1,1}. Additionally, the quinoline nitrogen is directed toward Lys^{1003}, although the distance to this residue may be too great to allow an H-bonding interaction. The 3-position of the quinoline is proximal to Val^{983}. In this binding mode, we do not observe the urea linkage making specific contacts with residues in the ATP binding site. Our current scaffolds lack useful hydrogen-bond interactions with the Glu^{1050} and Met^{1052} polar backbone atoms in the IGF-1R hinge region, which we hope to target in a future set of inhibitors.

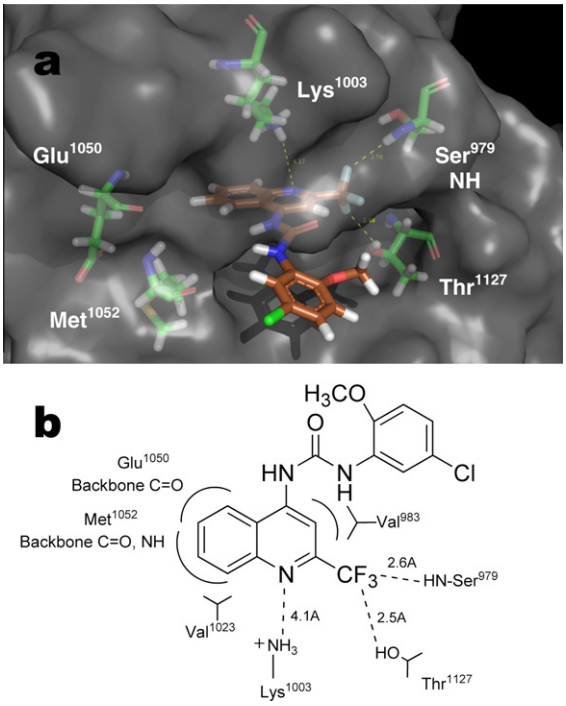

Figure 4. Computational docking of the relatively potent AHU inhibitor **2**{2,1} into the active site of IGF-1R kinase. (a) Three-dimensional side-view of postulated inhibitor–protein complex; (b) two-dimensional diagram showing key interactions with the ATP-binding site of IGF-1R. This inhibitor orientation will be referred to as 'Binding Mode A'.

When the entire set of AHU compounds was docked into the IGF-1R kinase structure, the binding mode could be classified in three possible ways (Table 2). The first mode (A) is consistent with the pose described in Figure 4 for inhibitor **2**{2,1}. The second binding mode (B) has the substituted aromatic ring projecting into the ATP-binding site, and the quinoline projecting out of the cavity. The third binding mode (C) is analogous to binding mode A, except that the orientation of the quinoline is flipped, that is, C_5–C_8 are projecting towards Val^{983}, and away from Glu^{1050} and Met^{1052}. Presented in Supplementary data are two relatively less potent inhibitors: **2**{3,8} adopting Binding Mode B; and **2**{5,10} adopting Binding Mode C (Figs. S1 and S2, respectively).

Interestingly, it appears that when the inhibitors are sorted from most potent to least potent, the more potent collection of inhibitors (IC_{50} <10 μM) appears to select lowest-energy binding mode A, with the exception of inhibitor **2**{4,1}. The less potent inhibitors (IC_{50} >10 μM) appear to adopt a more variable selection of the binding modes A–C. On the outset, our model suggests that the most potent AHU inhibitors adopt a consistent binding mode (A), which will be useful as we plan the rational design of future inhibitors. Further validation of binding mode A, through X-ray diffraction crystallography, is currently underway.

3. Conclusion

A lead aromatic heteroaryl urea structure **2**{1,1} was used as a starting point for optimization to improve inhibitory activity against IGF-1R. The general strategy was the replacement of the 4-aminoquinaldine system with other analogous ring systems that preserve the key heteroaromatic nitrogen atom. An additional strategy was the incorporation of novel substituted aromatic rings that contain tethered heterocycles which could improve the drug-like characteristics of the inhibitors. The results of this study are summarized in Figure 5. One promising alternative to the 4-aminoquinaldine heterocycle is 4-amino-2-trifluoromethylquinoline, which produced a new compound **2**{2,1} with fivefold potency improvement compared to lead structure **2**{1,1}. The presence of the aryl-linked 2-methylpyrazine substituted arene enhanced

Table 2
Inhibitors sorted by in vitro potency (IC_{50}) along with the computationally-determined lowest-energy binding mode (see text)

Compound	Minimum energy binding mode determined by docking (see text)	IGF-1R in vitro kinase inhibition (IC_{50} μM)
Compounds with IC_{50} below 10.0 μM:		
2{2,1}	A	3.5
2{2,10}	A	5.2
2{1,10}	A	5.6
2{4,1}	B	6.5
2{2,5}	A	6.7
2{2,2}	A	8.8
Compounds with IC_{50} above 10.0 μM:		
2{5,10}	C	12.5
2{1,3}	B	13.9
2{3,1}	A	14.9
2{2,6}	A	15.4
2{1,1}	A	18.7
2{2,8}	B	19.3
2{6,1}	B	20.5
2{3,4}	B	21.1
2{3,5}	B	21.4
2{5,1}	C	24.7
2{2,7}	C	27.1
2{2,4}	B	28.1
2{1,2}	A	>30
2{1,4}	B	>30
2{1,5}	B	>30
2{1,8}	C	>30
2{1,9}	B	>30
2{2,3}	A	>30
2{2,9}	C	>30
2{3,2}	A	>30
2{3,3}	C	>30
2{3,8}	B	>30
2{3,9}	A	>30
2{3,10}	B	>30
2{7,1}	A	>30

Binding modes: A = quinoline bound into the ATP-binding site with the quinoline N_1 atom proximal to Lys^{1003}, C_7 near Glu^{1050}, and the C_2-substituent (methyl, etc.) proximal to Ser^{979} (Fig. 4); B = a backward inhibitor binding mode with the substituted aromatic ring docked into the ATP binding site, and the quinoline is projected toward exposed solvent (Fig. S1); C = an alternative binding mode to A in which the quinoline is projected into the ATP binding site, but its orientation is flipped, or otherwise noticeably inconsistent with mode A (Fig. S2).

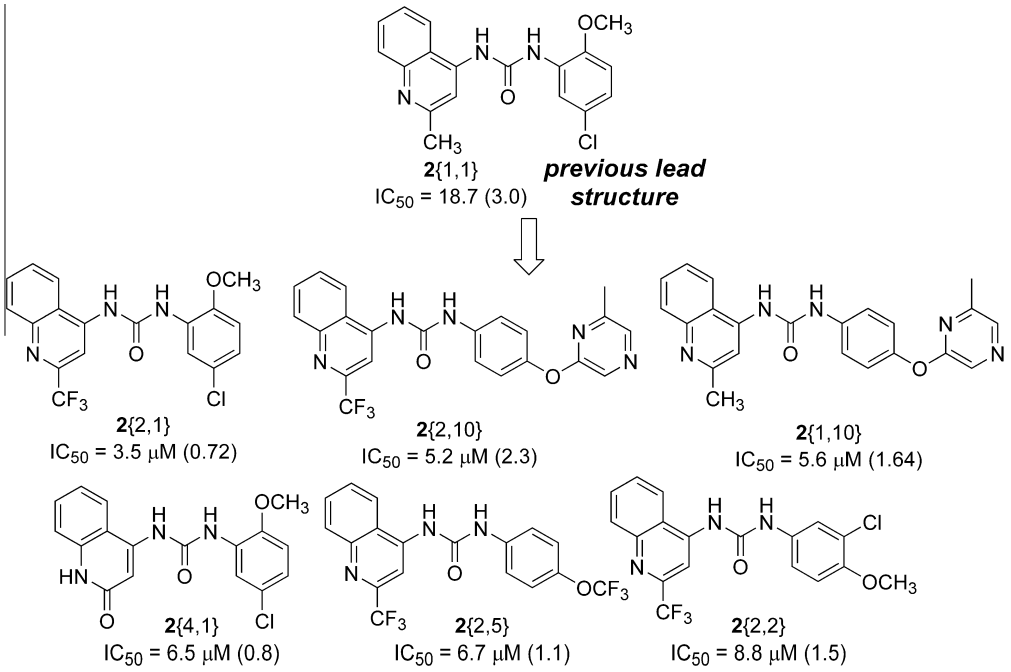

Figure 5. Summary of most potent compounds identified in this study, with in vitro kinase potency indicated (μM), with error in parenthesis.

potency in two inhibitors **2**{1-2,10}, which provided relatively low *c* Log *P* values, we suspect due to the presence of hydrogen-bond accepting heteroatoms. Compound **2**{4,1}, based on 4-amino-2-oxoquinoline showed promising inhibitory activity but preparing additional analogs was prevented due to purification issues. Inhibitors based on 4-amino-2-chloroquinoline, 4-amino-1,7 and 1,8-napthyridine were not particularly promising, but the novel syntheses of the parent heterocycles was provided. Lastly, a computational docking model of the more potent series of inhibitors was presented, showing that these compounds typically adopt a consistent mode of binding (mode 'A'), while the less-potent compounds do not adopt a consistent mode of binding. The computational modeling of these compounds has allowed us to plan the next step of rational design of inhibitors in this class. Our current working hypothesis is that by modifying the current quinoline-based inhibitors to incorporate polar functionalities (e.g., primary amide) positioned to interact with Glu^{1050} and Met^{1052}, we will be able to obtain inhibitors with enhanced potency. Results of these studies will be presented in due course.

4. Experimental

4.1. Synthesis

All solvents used in reactions were anhydrous and obtained as such from commercial sources. All other reagents were used as supplied unless otherwise stated. Liquid flash column chromatography was the procedure described by Still et al.[36] ^1H and ^{13}C NMR spectra were recorded on either a Bruker DRX 300 MHz or Bruker Avance 500 MHz spectrometer. ^1H NMR chemical shifts are relative to TMS (δ = 0.00 ppm), $CDCl_3$ (δ = 7.26 ppm), CD_3OD (δ = 4.87 and 3.31 ppm), or D_2O (δ = 4.87). ^{13}C NMR chemical shifts are relative to CD_3OD (δ = 49.15 ppm) or $CDCl_3$ (δ = 77.23 ppm). Analytical and semi-preparative HPLC was performed using a Dionex Ultimate 3000 system with either Higgins Analytical Targa C_{18} 150 × 4.6 mm columns (at 1 ml/min) or a YMC C_{18} 50 × 20 mm column (at 20 ml/min), respectively. High resolution mass spectra were obtained by the University of Notre Dame Mass Spectrometry and Proteomics Facility, Notre Dame, IN 46556-5670 using ESI either by direct infusion on a Bruker micrOTOF-II or by LC elution via an ultra-high pressure Dionex RSLC with C18 column coupled with a Bruker micrOTOF-Q II.

4.2. Computational modeling

The collection of inhibitors (Table 1, entries 1–32) was initially drawn in ChemDraw (Cambridge Software), and converted to a set of SMILES strings, which was then transformed to a library of single 3D conformations using OMEGA (OpenEyes). The single conformations were passed through MOLCHARGE (OpenEyes) in order to apply AM1BCC charges to each compound. Lastly, the charged set of compounds was passed once again through OMEGA (OpenEyes) to generate multi-conformational libraries for each compound. The neutral protonation state of the inhibitors generated by OMEGA was verified using the PKA plugin implemented in MarvinView (ChemAxon). *c* Log *P* values were calculated by the LOGP plugin implemented in JChem/MarvinView (ChemAxon). The protein receptor was prepared for docking with the FRED-RECEPTOR (OpenEyes) utility, employing a 2.00 Å resolution X-ray crystal structure of the unactivated IGF-1R kinase domain co-crystallized with an ATP-mimic inhibitor (PDB = 2OJ9).[33] To generate the receptor, the co-crystallized inhibitor was removed using PYMOL (DeLano Scientific), and the active site was then defined to be a 6 Å box around ATP binding site of the protein.

Upon successful preparation of the library of inhibitors and the receptor structure, docking was then performed using FRED (v2.2.5) (OpenEyes). FRED was configured to employ consensus scoring, with its full suite of scoring functions: ChemGauss3, OEChemScore, ScreenScore, PLP, and ZapBind. Docking of inhibitors was carried out free of pharmacophore restraints. Each final pose was minimized by FRED by molecular dynamics using the in the MMFF94 force field within the protein active site. The docking results, for each inhibitor, were sorted by top consensus score. The final protein–ligand complexes were visualized using PYMOL (DeLano Scientific).

4.3. In vitro IGF-1R inhibition screening

Inhibition of IGF-1R substrate kinase activity was determined by ELISA employing recombinant IGF-1R kinase domain proteins and biotin conjugated IRS-1 peptide substrate (Cell Signaling Technology, Inc.). IGF-1R (15 ng) were incubated with varying concentrations of AHU compounds for 5 min. IRS-1 sequence peptide (0.3 μM) was then added with 15 μM ATP under final buffer conditions of 60 mM HEPES, pH 7.5, 5 mM $MgCl_2$, 5 mM $MnCl_2$, 3uM Na_3VO_4. After 60 minutes the reaction was stopped by the addition of 50 mM EDTA. Next, the substrate was captured from a 50 μL aliquot of the reaction mixture added to a streptavidin-coated 96 well plate. After the substrate was allowed to bind to the plate, phosphorylation was determined by anti-phosphotyrosine antibody conjugated to HRP.

4.3.1. 4-Azido-2-trifluoromethylquinoline (7)

To a 40 ml scintillation vial was added 4-chloro-2-trifluoromethylquinoline (400 mg, 1.73 mmol) (**6**), 1-butanol (4 ml), sodium azide (1.1 g, 17.3 mmol, 10 equiv), and 15-crown-5 (0.342 ml, 1.73 mmol, 1 equiv). The vial was sealed and heated to 150 °C while stirring. After 4 h, RP-HPLC showed consumption of SM and formation of product. The reaction mixture was dry-loaded onto Celite, and was then purified by silica-gel flash column chromatography [hexane→25:1 hexanes/ethyl acetate + 0.05% triethylamine] to generate the title compound as a colorless film (302.6 mg, 76%). The compound was rapidly advanced to the next step to avoid photochemical degradation. ^1H NMR ($CDCl_3$, 500 MHz): δ 7.41 (s, 1 H) 7.64 (t, *J* = 7.57 Hz, 1 H), 7.82 (t, *J* = 5 Hz, 1H), 8.09 (d, *J* = 8.20 Hz, 1H), 8.16 (d, *J* = 8.51 Hz, 1H). ^{13}C NMR ($CDCl_3$, 125 MHz): δ 105.1, 122.6, 123.0, 129.1, 130.6, 132.4, 148.85 (q, *J* = 13.75 Hz).

4.3.2. 4-Amino-2-trifluoromethyl-quinoline 3{2}

A portion of 4-azidotrifluoromethylquinoline (**7**) (302 mg, 1.27 mmol) was dissolved in MeOH (18 ml), treated with Pd (10% on carbon) (0.1 equiv), and stirred under argon. The vessel was subjected twice to evacuation followed by purging with a hydrogen balloon, and then allowed to stir under hydrogen for 3 h. TLC showed consumption of starting material and formation of product. The reaction mixture was filtered through a bed of Celite and then concentrated in vacuo to yield the product as a slightly yellow solid (269 mg, 73%), which is a commercially available material. Mp = 138–140 °C. ^1H NMR (CD_3CN, 500 MHz): δ 5.90 (br s, 1H), 6.88 (s, 1H), 7.49 (t, *J* = 10 Hz, 1H), 7.66 (t, *J* = 10 Hz, 1H) 7.87 (d, *J* = 8.51 Hz, 1H), 7.92 (d, *J* = 10 Hz, 1H). ^{13}C NMR (CD_3CN, 125 MHz): δ 98.7, 118.0, 119.3, 112.2, 126.7, 130.3, 131.2, 148.8, 153.8. LC-ESI(+)-TOF-HRMS $(M+H)^+$ calcd 213.0639 found 213.0642 for $C_{10}H_7F_3N_2$.

4.3.3. General conditions for coupling aminoquinoline derivatives 3{a} to substituted aromatic isocyanates 4{b} to generate AHU compounds 2{a,b}

An appropriate 4-aminoquinoline derivative **3**{a} was dissolved in DMSO (0.1 M), treated with sodium *tert*-butoxide (2.0 equiv only for aminoquinolines **3**{2}, **3**{3}, and **3**{4}), and stirred 15 min, usually causing the solution to turn slightly brown. Subsequently, the solution was treated with an aromatic isocyanate **4**{b} (1.0–1.2 equiv)

and stirred 30 min at rt, with the progress of the reaction followed by RP-HPLC analysis. The products were purified by precipitation by addition to water/AcOH (1:1), NaOH (0.1 M aq), or directly purified by semi-preparative RP-HPLC using a Dionex Ultimate 3000 instrument.

4.3.4. 4-Chloro-2-methyl-1,8-naphthyridine (11)

A 60 ml scintillation vial with a polypropylene-lined cap was charged with 2-aminonicotinic acid (**13**) (1000 mg) and acetone (2 ml, 4 equiv), and the reaction mixture was allowed to stand for ca. 5 min before being treated with $POCl_3$ (35 ml, 0.2 M). The reaction mixture was then heated for 5.5 h at 80 °C. Next, the reaction mixture was carefully added to 200 ml ice water, which was then basified to pH 14 with NaOH (6 M aq) and stirred for 40 min (with additional base added to maintain pH 14). The aqueous material was split into two portions. Each portion was extracted with DCM (6 × 100 ml). The organic layers were combined and concentrated in vacuo to generate crude product (**11**) (0.727 g, 56%) which was employed directly in the next step without further purification or characterization.

4.3.5. 4-Azido-2-methyl-1,8-naphthyridine (15)

A solution of crude 4-chloro-2-methyl-1,8-naphthyridine (**11**) (727 mg, 4.0 mmol) was dissolved in MeOH (20 ml) and treated with sodium azide (2.6 g, 40.7 mmol, 10.2 equiv) and 15-crown-5 (0.040 ml, 0.407 mmol, 0.05 equiv). The mixture was heated to 80 °C for 18 h, and then RP-HPLC analysis was used to determine that the reaction has proceeded quantitatively. The reaction mixture was dry-loaded onto Celite, and was then purified by silica-gel flash column chromatography (eluted with EtOAc) to generate the title compound as a white film (548 mg, 73%). The compound was rapidly advanced to the next step to avoid photochemical degradation. ^{1}H NMR ($CDCl_3$, 500 MHz): δ 2.78 (s, 3H), 7.06 (s, 1H) 7.39 (dd, J = 8.20, 4.41 Hz, 1 H), 8.32 (dd, J = 8.20, 1.89 Hz, 1H), 9.06 (d, J = 5 Hz). ^{13}C NMR ($CDCl_3$, 125 MHz): δ 25.8, 109.9, 114.7, 121.0, 131.6, 146.8, 154.2, 156.7, 162.8.

4.3.6. 4-Amino-2-methyl-1,8-naphthyridine 3{5}

A solution of 4-azido-2-methyl-1,8-naphthyridine (**15**) (20 mg, 0.108 mmol) was dissolved in MeOH (1 ml) was treated with sodium borohydride (8 mg, 0.216 mmol, 2 equiv) and then heated to 40 °C for 20 min whereupon fairly intense bubbling occurred. TLC indicated consumption of starting material and formation of suspected product. To destroy boron complexes, H_2O (10 ml) was added, and then the pH was set to 1 with HCl (1 M aq), and then the mixture was re-basified to pH 14 with NaOH (6 M aq). The solution was extracted with DCM (2 × 20 ml), the organic layer was dried over Na_2SO_4, and concentrated in vacuo to yield the product **3**{5} as a slightly orange solid (18 mg, quantitative yield). Mp = 190–200 °C (dec). IR (cm^{-1}, KBr): 1596, 1662, 3060. ^{1}H NMR (MeOH-d_4, 500 MHz): δ 2.53 (s, 3H), 6.59 (s, 1H), 7.38 (dd, J = 8.20, 4.41 Hz, 1H), 8.52 (dd, J = 8.35, 1.73 Hz, 1H), 8.84–8.85 (mult, 1H). ^{13}C NMR (MeOH-d_4, 125 MHz): δ 25.2, 104.3, 113.3, 120.2, 133.7, 153.8, 155.4, 157.8, 163.8. LC-ESI(+)-TOF-HRMS $(M+H)^+$ calcd 160.0874, found 160.0871 for $C_9H_9N_3$.

4.3.7. 2-Methyl-5,6,7,8-tetrahydro-[1,8]naphthyridin-4-ylamine 3{6}

A solution of crude 4-azido-2-methyl-1,8-naphthyridine (**15**) (187 mg, 1.150 mmol) was dissolved in MeOH (11 ml) was treated with platinum oxide (26 mg, 0.115 mmol, 0.1 equiv), and stirred under argon. The vessel was subjected twice to evacuation followed by purging with a hydrogen balloon, and then allowed to stir under hydrogen for 18 h. RP-HPLC analysis showed consumption of starting material and formation of suspected product. The reaction mixture was filtered through a bed of Celite and then concentrated in vacuo to yield the product as a white waxy solid film (186 mg, 99%). ^{1}H NMR (MeOH-d_4, 500 MHz): δ 1.90 (p, J = 5 Hz, 2H), 2.13 (s, 3H), 2.39 (t, J = 10 Hz, 2H), 3.26–3.28 (mult, 2H), 3.31 (mult, 1H), 5.88 (s, 1H). ^{13}C NMR (MeOH-d_4, 125 MHz): δ 21.5, 22.7, 22.8, 42.1, 96.5, 102.0, 152.9, 155.03, 156.64. LC-ESI(+)-TOF-HRMS $(M+H)^+$ calcd 164.1187, found 164.1193 for $C_9H_{13}N_3$.

4.3.8. 4-Chloro-2-methyl-1,7-naphthyridine (17)

3-Aminoisonicotinic acid (**16**) (50 mg, 0.362 mmol) was treated with acetone (0.133 ml, 1.81 mmol, 5 equiv) and allowed to stand for 5 min. The reaction mixture was then carefully treated with $POCl_3$ (20 ml), and then heated at 100 °C under air for 60 min. RP-HPLC analysis showed consumption of starting material and formation of suspected product. The reaction mixture was transferred to a beaker containing 200 ml ice water, and the contents were subsequently basified to pH 14 using NaOH solution (5 N aq), and then treated with NaCl (satd aq) to 'salt out' the organic product. The organic material was extracted with DCM (3 × 50 ml), dried over Na_2SO_4, and concentrated in vacuo to generate the crude product. The material was then purified by flash column chromatography (1:1 hexanes/EtOAc) to generate the product (**17**) (22 mg, 35%) as an off-color film, which has been previously characterized.[37] ^{1}H NMR (MeOH-d_4, 500 MHz): δ 2.75 (s, 3H), 7.82 (s, 1H), 8.04 (d, J = 5.67 Hz, 1H), 8.61 (d, J = 5.99 Hz, 1H) 9.27 (s, 1H). ^{13}C NMR (MeOH-d_4, 125 MHz): δ 24.3, 117.1, 126.9, 129.1, 142.2, 143.6, 143.9, 152.8, 162.8. LC-ESI(+)-TOF-HRMS $(M+H)^+$ calcd 179.0376, found 179.0382 for $C_9H_7ClN_2$.

4.3.9. 4-Azido-2-methyl-1,7-naphthyridine (18)

A solution of 4-chloro-2-methyl-1,7-naphthyridine(**17**) (10.8 mg) in 1-propanol (1.8 ml) was treated with 15-crown-5 (0.024 ml, 0.122 mmol) and sodium azide (40.5 mg, 0.607 mmol, 10 equiv). The reaction mixture was stirred at 120 °C overnight. RP-HPLC analysis showed conversion of starting material to product. The material was purified by flash column chromatography (40:1 dichloromethane/MeOH) to generate the product (**18**) (5.9 mg, 53%) as a slightly yellow film. The compound was rapidly advanced to the next step to avoid photochemical degradation. IR (cm^{-1}, KBr): 1593, 1665, 2922. ^{1}H NMR (MeOH-d_4, 500 MHz): δ 2.76 (s, 3H), 7.85 (s, 1H), 8.07 (d, J = 5.7 Hz, 1H), 8.63 (d, J = 5.67 Hz, 1 H), 9.29 (s, 1H). ^{13}C NMR (MeOH-d_4, 125 MHz): δ 24.5, 114.2, 115.7, 124.5, 142.9, 143.7, 147.0, 152.0, 162.9.

4.3.10. 4-Amino-2-methyl-1,7-naphthyridine 3{7}

A solution of 4-azido-2-methyl-1,8-naphthyridine (**18**) (120 mg, 0.6408 mmol) in methanol (6.5 ml) was treated with platinum oxide (21.1 mg, 0.093 mmol, 0.15 equiv), and stirred under argon. The vessel was subjected twice to evacuation followed by purging with a hydrogen balloon, and then allowed to stir under hydrogen for 90 min. The reaction mixture was filtered through a bed of Celite and then concentrated in vacuo to yield the product as a yellow oil (97.7 mg, 95%). ^{1}H NMR (MeOH-d_4, 500 MHz): δ 2.54 (s, 3H), 6.69 (s, 1H), 7.95 (d, J = 5.67 Hz, 1H), 8.35 (d, J = 5.67 Hz, 1H), 9.04 (s, 1H). ^{13}C NMR (MeOH-d_4, 125 MHz): δ 24.07, 105.5, 116.0, 122.1, 140.5, 144.0, 151.4, 152.5, 162.0. LC-ESI(+)-TOF-HRMS $(M+H)^+$ calcd 160.0874, found 160.0873 for $C_9H_9N_3$.

4.3.11. 2,4-Dichloroquinoline (23)

To a 20 ml scintillation vial was added 2,4-dihydroxyquinoline (**22**) (200 mg, 1.24 mmol), which was then carefully treated with $POCl_3$ (4.2 ml, 0.3 M) and the reaction was then heated to 100 °C for 2 h. RP-HPLC analysis showed consumption of starting material and formation of suspected product. The reaction mixture was transferred to a beaker containing ice water (100 ml) and NaOH (6 M, 35 ml), and then stirred to quench unreacted $POCl_3$. The product was then extracted with diethyl ether (3 × 50 ml) and

then the combined organic material was washed with NaCl (satd aq) (50 ml), dried over Na_2SO_4, and concentrated in vacuo to yield the product (**23**) (221 mg, 90% yield). The compound has been prepared previously[38] and is also commercially available. ^{1}H NMR ($CDCl_3$, 500 MHz): δ 7.49 (s, 1H), 7.64 (t, J = 7.72 Hz, 1H), 7.78 (t, J = 10 Hz, 1H), 8.02 (d, J = 8.51 Hz, 1H), 8.17 (d, J = 10 Hz, 1H). LC-ESI(+)-TOF-HRMS $(M+H)^+$ calcd 197.9877, found 197.9881 for $C_9H_5Cl_2N$.

4.3.12. 4-Chloro-1*H*-quinolin-2-one (24)

A solution of 2,4-dichloroquinoline (**23**) (979 mg, 4.94 mmol) in HCl (6 M):dioxane (1.4:1) was heated to 90 °C for 5 h. RP-HPLC analysis showed consumption of starting material and formation of product. Solid K_2CO_3 was carefully added to the reaction mixture until the pH was 9. The solution was extracted with EtOAc/Et_2O (1:1) (6 × 100 ml), and the combined organic layer was washed with NaCl (satd aq), dried over Na_2SO_4, and concentrated in vacuo to yield the product (499 mg, 56%). The compound has been prepared previously[39] and is also commercially available. IR (cm^{-1}, KBr): 1664, 2847. ^{1}H NMR (DMSO-d_6, 500 MHz): δ 6.83 (s, 1H), 7.31 (t, J = 7.57 Hz, 1H), 7.39 (d, J = 8.20 Hz, 1H), 7.63 (t, J = 7.72 Hz, 1H), 7.86 (d, J = 8.20 Hz, 1H), 12.05 (br s, 1H). LC-ESI(+)-TOF-HRMS $(M+H)^+$ calcd 180.0216, found 180.0218 for C_9H_6ClNO.

4.3.13. 4-Azido-1H-quinolin-2-one (25)

A solution of 4-chloro-1H-quinolino2-one (**24**) (480 mg, 2.67 mmol) in DMF (10 ml) was treated with sodium azide (1.7 g, 26.7 mmol, 10 equiv) and 15-crown-5 (0.529 ml, 2.67 mmol, 1.0 equiv), and then the solution was allowed to stir at 100 °C for 20 h. RP-HPLC analysis showed almost complete (~90%) conversion to product. The reaction mixture was diluted with H_2O (350 ml), and the product was extracted with EtOAc/Et_2O (1:1) (3 × 120 ml). The organic mixture was dried over Na_2SO_4, and concentrated in vacuo to generate 4-azido-1*H*-quinolin-2-one, which was purified by flash column chromatography (hexane/EtOAc (1:2)→hexane/EtOAc (1:2) + 1% triethylamine) yielding the desired product (366 mg, 73%) as a white solid. The compound was rapidly advanced to the next step to avoid photochemical degradation. The compound has been prepared previously[40] and is also commercially available. ^{1}H NMR (DMSO-d_6, 500 MHz): δ 6.36 (s, 1H), 7.19 (t, J = 10 Hz, 1H), 7.57 (td, J = 7.73, 1.37 Hz, 1H), 7.68 (d, J = 15 Hz, 1H). LC-ESI(+)-TOF-HRMS $(M+H)^+$ calcd 187.0620, found 187.0622 for $C_9H_6N_4O$.

4.3.14. 4-Amino-1H-quinolin-2-one 3{4}

A solution of 4-azido-1*H*-quinolin-2-one (25 mg, 0.134 mmol) (**25**) in MeOH (1.5 ml) was treated with palladium (10% on carbon) (14 mg, 0.013 mmol) and stirred under argon. The vessel was subjected twice to evacuation followed by purging with a hydrogen balloon, and then allowed to stir under hydrogen for 3 h. The reaction mixture was filtered through a bed of Celite and then concentrated in vacuo to yield the final product **3**{4} product as a light grey solid (20 mg, 97%). The compound has been prepared previously[40] and is also commercially available. Mp = 260–265 °C (dec). IR (cm^{-1}, KBr): 1636, 3130. ^{1}H NMR (DMSO-d_6, 500 MHz): δ 5.40 (s, 1H), 6.54 (br s, 2H), 7.06 (t, J = 10 Hz, 1H), 7.18 (dd, J = 8.23, 1.10 Hz, 1H), 7.41 (ddd, J = 8.28, 7.09, 1.28 Hz, 1H), 7.84 (dd, J = 8.14, 1.01 Hz, 1H), 10.71 (br s, 1H). LC-ESI(+)-TOF-HRMS $(M+H)^+$ calcd 161.0715, found 161.0714 for $C_9H_8N_2O$.

4.3.15. 2-Chloro-quinolin-4-ylamine 3{3}

A solution of 4-azido-1*H*-quinolin-2-one (20 mg, 0.107 mmol) (**25**) in $POCl_3$ (1.5 ml) was heated to 100 °C for 2 h. RP-HPLC analysis showed conversion of starting material to product. The reaction mixture was carefully added to a beaker containing ice water (100 ml) and NaOH (6 M) (15 ml). The mixture was stirred for 30 min while more base was added to maintain the pH at 14. The aqueous material was extracted with Et_2O/EtOAc (4 × 40 ml), and the resultant organic layer was dried over Na_2SO_4 and concentrated in vacuo to yield 4-azido-2-chloro-quinoline (20.0 mg, 91%) which was used in the next step without further purification. A solution of 4-azido-2-chloro-quinoline (20 mg, 0.098 mmol) in MeOH (1 ml) was treated with sodium borohydride (3.7 mg, 0.098 mmol), and stirred at rt for 30 min. HPLC showed conversion of starting material to tentative product. The mixture was treated with HCl (1 M aq, 10 ml) to quench borohydride, and was then basified with to pH 9 with NaOH (1 M), and then extracted with CH_2Cl_2 (3 × 10 ml). The organic layer was concentrated in vacuo to yield the final product (13.4 mg, 77%). The compound has been prepared previously[38] and is also commercially available. ^{1}H NMR (CD_3OD, 300 MHz): δ 6.58 (s, 1H), 7.40–7.46 (mult, 1H), 7.56–7.77 (mult, 2H), 8.03 (d, J = 9 Hz, 1H). ^{13}C NMR (DMSO-d_6, 125 MHz): δ 100.5, 117.6, 122.5, 124.3, 127.9, 130.3, 148.0, 150.6, 154.1. LC-ESI(+)-TOF-HRMS $(M+H)^+$ calcd 179.0376, found 179.0381 for $C_9H_7ClN_2$.

Acknowledgments

This work was supported in part by a grant from the National Institutes of Health (R01 CA-112042-01 A1). Terrance O'Brien received funding from the NIH-MARC program (T34-GM08574). Megumi Tamaki is acknowledged for the re-synthesis and purification of several inhibitors. Mass spectroscopy services at SFSU were funded by grants from the National Institutes of Health (P20 MD00544) and the National Science Foundation (CHE-0619163), utilizing the services of Dr. Robert Yen. The authors would also like to extend their gratitude to Wee Tam at the SFSU NMR facility for his expert assistance. Mass-spectrometry services at University of Notre Dame were supported by grants from the National Science Foundation (CHE-0741793). Lastly, the authors would like to acknowledge OpenEyes Inc. and ChemAxon Inc. for providing free site licenses to the academic community.

Supplementary data

Supplementary data associated with this article can be found, in the online version, at doi:10.1016/j.bmc.2010.06.071.

References and notes

1. Yuen, J. S.; Macaulay, V. M. *Expert Opin. Ther. Targets* **2008**, *12*, 589.
2. Bruchim, I.; Attias, Z.; Werner, H. *Expert Opin. Ther. Targets* **2009**, *13*, 1179.
3. Hofmann, F.; Garcia-Echeverria, C. *Drug Disc. Today* **2005**, *10*, 1041.
4. Garcia-Echeverria, C. *IDrugs* **2006**, *9*, 415.
5. Baker, J.; Liu, J. P.; Robertson, E. J.; Efstratiadis, A. *Cell* **1993**, *75*, 73.
6. Liu, J. P.; Baker, J.; Perkins, A. S.; Robertson, E. J.; Efstratiadis, A. *Cell* **1993**, *75*, 59.
7. Samani, A. A.; Yakar, S.; LeRoith, D.; Brodt, P. *Endocr. Rev.* **2007**, *28*, 20.
8. Baserga, R.; Peruzzi, F.; Reiss, K. *Int. J. Cancer* **2003**, *107*, 873.
9. LeRoith, D.; Helman, L. *Cancer Cell.* **2004**, *5*, 201.
10. Mazitschek, R.; Giannis, A. *Curr. Opin. Chem. Biol.* **2004**, *8*, 432.
11. Morin, M. J. *Oncogene* **2000**, *19*, 6574.
12. Hendrickson, A. W.; Haluska, P. *Curr. Opin. Investig. Drugs* **2009**, *10*, 1032.
13. Gualberto, A.; Karp, D. D. *Clin. Lung Cancer* **2009**, *10*, 273.
14. Tolcher, A. W.; Sarantopoulos, J.; Patnaik, A.; Papadopoulos, K.; Lin, C. C.; Rodon, J.; Murphy, B.; Roth, B.; McCaffery, I.; Gorski, K. S.; Kaiser, B.; Zhu, M.; Deng, H.; Friberg, G.; Puzanov, I. *J. Clin. Oncol.* **2009**, *27*, 5800.
15. Durai, R.; Yang, S. Y.; Sales, K. M.; Seifalian, A. M.; Goldspink, G.; Winslet, M. C. *Colorectal. Dis.* **2007**, *9*, 625.
16. Yin, D.; Vreeland, F.; Schaaf, L. J.; Millham, R.; Duncan, B. A.; Sharma, A. *Clin. Cancer Res.* **2007**, *13*, 1000.
17. Firth, S. M.; Baxter, R. C. *Endocr. Rev.* **2002**, *23*, 824.
18. Sarma, P. K. S.; Tandon, R.; Gupta, P.; Dastidar, S. G.; Ray, A.; Das, B.; Cliffe, I. A. *Expert Opinion on Therapeutic Patents*; Informa Healthcare, 2007. pp 25–35.
19. Hewish, M.; Chau, I.; Cunningham, D. *Recent Pat. Anticancer Drug Disc.* **2009**, *4*, 54.
20. Mitsiades, C. S.; Mitsiades, N. S.; McMullan, C. J.; Poulaki, V.; Shringarpure, R.; Akiyama, M.; Hideshima, T.; Chauhan, D.; Joseph, M.; Libermann, T. A.; Garcia-

Echeverria, C.; Pearson, M. A.; Hofmann, F.; Anderson, K. C.; Kung, A. L. *Cancer Cell.* **2004**, *5*, 221.
21. Munshi, S.; Hall, D. L.; Kornienko, M.; Darke, P. L.; Kuo, L. C. *Acta Crystallogr., Sect. D* **2003**, *59*, 1725.
22. Rodon, J.; DeSantos, V.; Ferry, R. J., Jr.; Kurzrock, R. *Mol. Cancer Ther.* **2008**, *7*, 2575.
23. Weroha, S. J.; Haluska, P. *J. Mammary Gland Biol. Neoplasia* **2008**, *13*, 471.
24. Garcia-Echeverria, C.; Pearson, M. A.; Marti, A.; Meyer, T.; Mestan, J.; Zimmermann, J.; Gao, J.; Brueggen, J.; Capraro, H. G.; Cozens, R.; Evans, D. B.; Fabbro, D.; Furet, P.; Porta, D. G.; Liebetanz, J.; Martiny-Baron, G.; Ruetz, S.; Hofmann, F. *Cancer Cell.* **2004**, *5*, 231.
25. Sabbatini, P.; Korenchuk, S.; Rowand, J. L.; Groy, A.; Liu, Q.; Leperi, D.; Atkins, C.; Dumble, M.; Yang, J.; Anderson, K.; Kruger, R. G.; Gontarek, R. R.; Maksimchuk, K. R.; Suravajjala, S.; Lapierre, R. R.; Shotwell, J. B.; Wilson, J. W.; Chamberlain, S. D.; Rabindran, S. K.; Kumar, R. *Mol. Cancer Ther.* **2009**, *8*, 2811.
26. Boyd, D. B. *Integr. Cancer Ther.* **2003**, *2*, 315.
27. Gupta, K.; Krishnaswamy, G.; Karnad, A.; Peiris, A. N. *Am. J. Med. Sci.* **2002**, *323*, 140.
28. Gable, K. L.; Maddux, B. A.; Penaranda, C.; Zavodovskaya, M.; Campbell, M. J.; Lobo, M.; Robinson, L.; Schow, S.; Kerner, J. A.; Goldfine, I. D.; Youngren, J. F. *Mol. Cancer Ther.* **2006**, *5*, 1079.
29. Anderson, M. O.; Yu, H.; Penaranda, C.; Maddux, B. A.; Goldfine, I. D.; Youngren, J. F.; Guy, R. K. *J. Comb. Chem.* **2006**, *8*, 784.
30. Mayer, S. C.; Banker, A. L.; Boschelli, F.; Di, L.; Johnson, M.; Kenny, C. H.; Krishnamurthy, G.; Kutterer, K.; Moy, F.; Petusky, S.; Ravi, M.; Tkach, D.; Tsou, H. R.; Xu, W. *Bioorg. Med. Chem. Lett.* **2008**, *18*, 3641.
31. Miller, L. M.; Mayer, S. C.; Berger, D. M.; Boschelli, D. H.; Boschelli, F.; Di, L.; Du, X.; Dutia, M.; Floyd, M. B.; Johnson, M.; Kenny, C. H.; Krishnamurthy, G.; Moy, F.; Petusky, S.; Tkach, D.; Torres, N.; Wu, B.; Xu, W. *Bioorg. Med. Chem. Lett.* **2009**, *19*, 62.
32. Wittman, M. D.; Carboni, J. M.; Yang, Z.; Lee, F. Y.; Antman, M.; Attar, R.; Balimane, P.; Chang, C.; Chen, C.; Discenza, L.; Frennesson, D.; Gottardis, M. M.; Greer, A.; Hurlburt, W.; Johnson, W.; Langley, D. R.; Li, A.; Li, J.; Liu, P.; Mastalerz, H.; Mathur, A.; Menard, K.; Patel, K.; Sack, J.; Sang, X.; Saulnier, M.; Smith, D.; Stefanski, K.; Trainor, G.; Velaparthi, U.; Zhang, G.; Zimmermann, K.; Vyas, D. M. *J. Med. Chem.* **2009**, *52*, 7360.
33. Velaparthi, U.; Wittman, M.; Liu, P.; Stoffan, K.; Zimmermann, K.; Sang, X.; Carboni, J.; Li, A.; Attar, R.; Gottardis, M.; Greer, A.; Chang, C. Y.; Jacobsen, B. L.; Sack, J. S.; Sun, Y.; Langley, D. R.; Balasubramanian, B.; Vyas, D. *Bioorg. Med. Chem. Lett.* **2007**, *17*, 2317.
34. Deady, L. W.; Werden, D. M. *Synth. Commun.* **1987**, *17*, 319.
35. Favelyukis, S.; Till, J. H.; Hubbard, S. R.; Miller, W. T. *Nat. Struct. Biol.* **2001**, *8*, 1058.
36. Still, W. C.; Kahn, M.; Mitra, A. *J. Org. Chem.* **1978**, *43*, 2923.
37. Yamashkin, S. A.; Kucherenko, N. Y.; Yurovskaya, M. A. *Chem. Heterocycl. Compd. (N. Y.)* **1997**, *33*, 499.
38. Heitman, L. H.; Goeblyos, A.; Zweemer, A. M.; Bakker, R.; Mulder-Krieger, T.; van, V. J. P. D.; de, V. H.; Brussee, J.; Ijzerman, A. P. *J. Med. Chem.* **2009**, *52*, 926.
39. van, O. A.; Motamedi, M.; Martinborough, E.; Zhao, S.; Shen, Y.; West, S.; Chang, W.; Kallel, A.; Marschke, K. B.; Lopez, F. J.; Negro-Vilar, A.; Zhi, L. *Bioorg. Med. Chem. Lett.* **2007**, *17*, 1527.
40. Aizikovich, A.; Kuznetsov, V.; Gorohovsky, S.; Levy, A.; Meir, S.; Byk, G.; Gellerman, G. *Tetrahedron Lett.* **2004**, *45*, 4241.